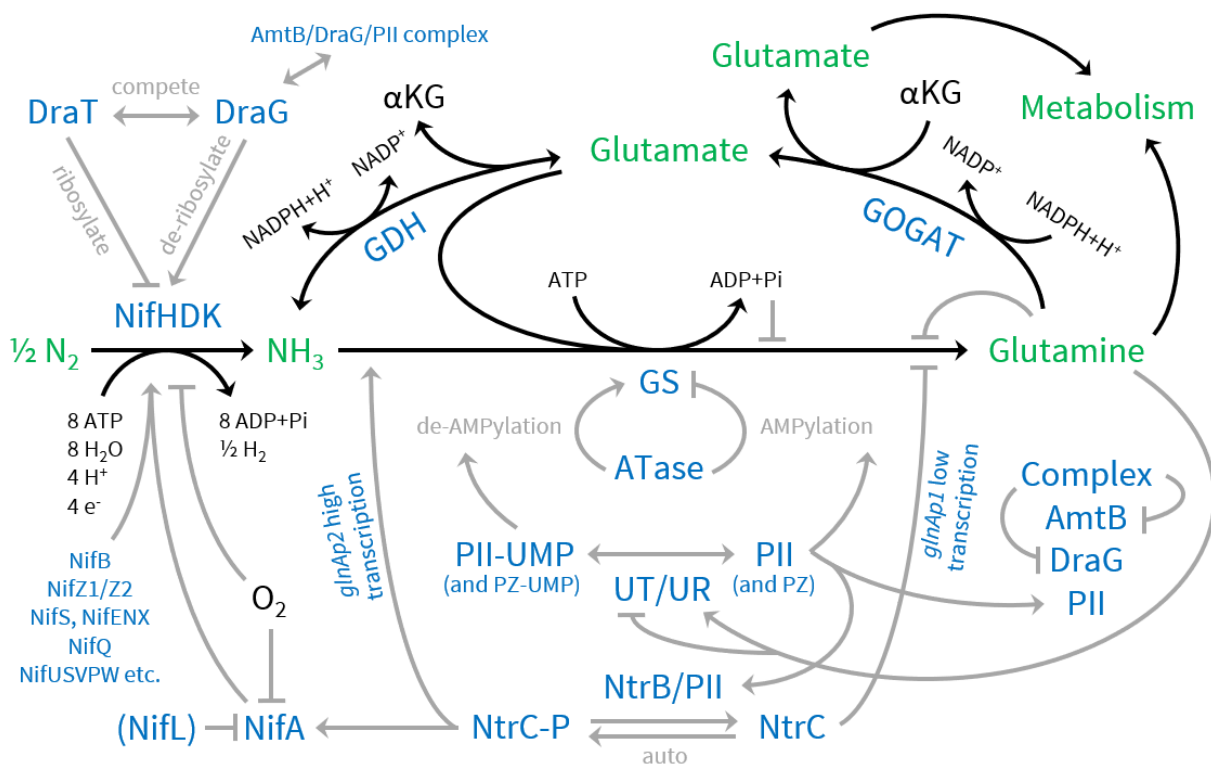


Engineering post-translational regulation of glutamine synthetase for controllable ammonia production in the plant-symbiont *A. brasilense*

Supplemental Materials

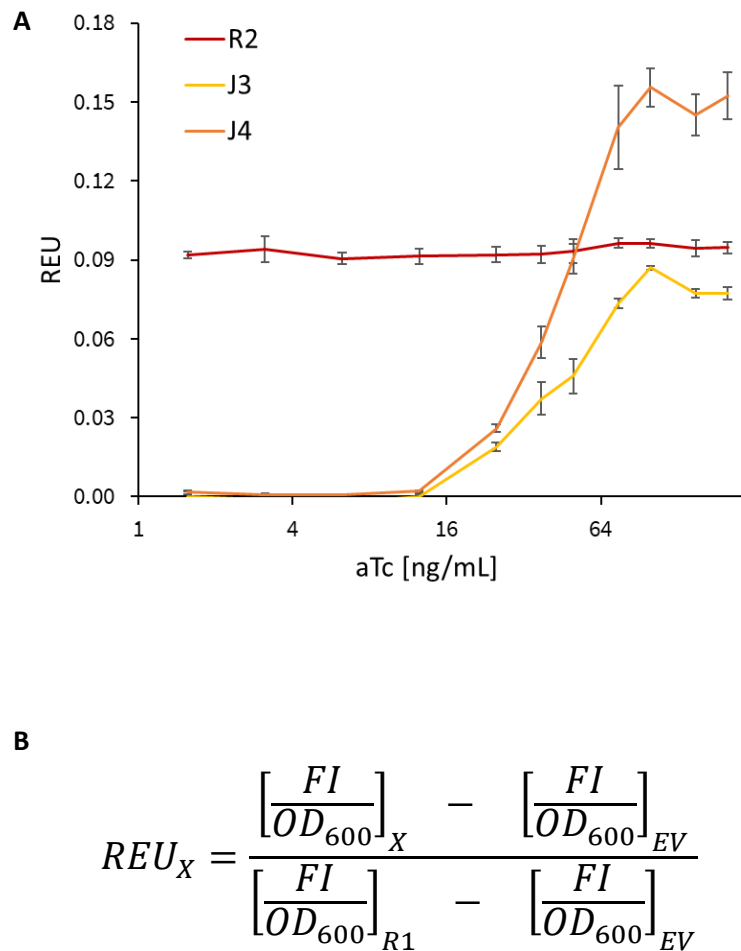
Figure S1: Schematic of complex nitrogen fixation feedback regulation in diazotrophs based on summary of findings reported in the primary literature.



Briefly: glutamine synthetase (GS, *glnA*) is post-translationally deactivated by adenylylation, modulated by ATase (glutamine synthetase adenylyltransferase, *glnE*). ATase can also reverse (hydrolyze) this modification to GS. The directionality (adenylyltransferring or adenylylremoving) and activity of ATase are

regulated by numerous mechanisms including but not limited to PII (*glnB*) and PZ (*glnZ*), which are key regulatory proteins responsive to the intracellular nitrogen status (1-4). Amongst others, by interacting with the histidine kinase/phosphatase activity of NtrB (*glnL*), PII and PZ affect the phosphorylation state and activity of NtrC (*glnG*), a central transcriptional regulator of numerous genes, including *glnA* encoding GS and *nifA* encoding the nitrogen fixation global transcriptional regulator that affects transcription of the nitrogenase complex NifHDK and many of its accessory *nif* genes(5, 6). Furthermore, PII and PZ form a complex with AmtB (ammonia membrane diffusion transporter) and DraG to affect nitrogenase ribosylation and ammonia sensing and possibly transport (7-10). DraG (nitrogenase ADP-ribosylhydrolase) opposes the activity of DraT (nitrogenase ADP-ribosyltransferase), which deactivates NifHDK by ribosylation. Furthermore, the activities of PII and PZ are in part controlled by their post-translational uridylylation state, which is in turn controlled by the bidirectional UT/UR (uridylyltransferring/uridylylremoving, *glnD*) based on intracellular nitrogen, carbon, and energy status (11). Usually PII and PZ are uridylylated under nitrogen starvation. The directionality and activity of ATase are also thought to be directly modulated by small molecules such as glutamine and alpha-ketoglutarate (α KG) that bind the regulatory region separating the adenylyltransferring and adenylylremoving domains (2, 3). NifL functions as an anti-activator to NifA in some species, such as *A. vinelandii*, and is itself under complex regulation not shown here(12). Other abbreviations: GDH (glutamate dehydrogenase, *gdhA*, *gdhB*), GOGAT (glutamine 2-oxoglutarate amidotransferase (glutamate synthase), *gltBD*).

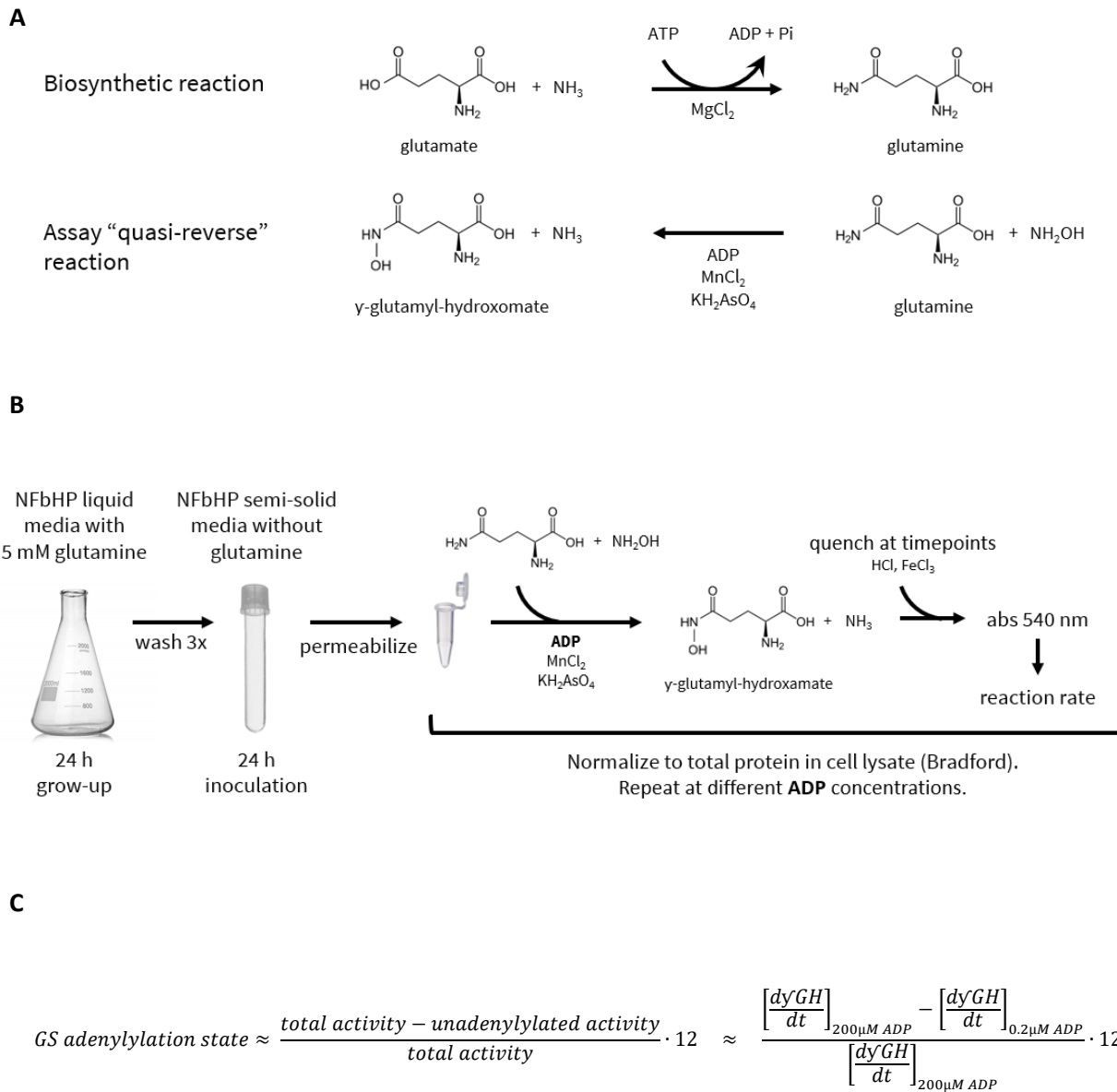
Figure S2: Testing genetic circuits in *A. brasiliense* through red fluorescent protein (RFP) readout.



[A] Genetic circuits were tested on pTS7 with circuit gene of interest (GOI) = RFP [see Fig S21 for diagrams and part sequences]. Cells were inoculated and induced with anhydrotetracycline (aTc) at OD₆₀₀ 0.5 in 200 µL volumes in a 96-well plate at 300 rpm and 30°C. OD₆₀₀ and fluorescence (575/15 excitation and 615/16 emission) were determined 48 h later and relative expression units (REUs) were calculated as shown in **[B]**. In the absence of standard genetic tools in *A. brasiliense*, the R1 circuit on pTS7 with GOI = RFP was

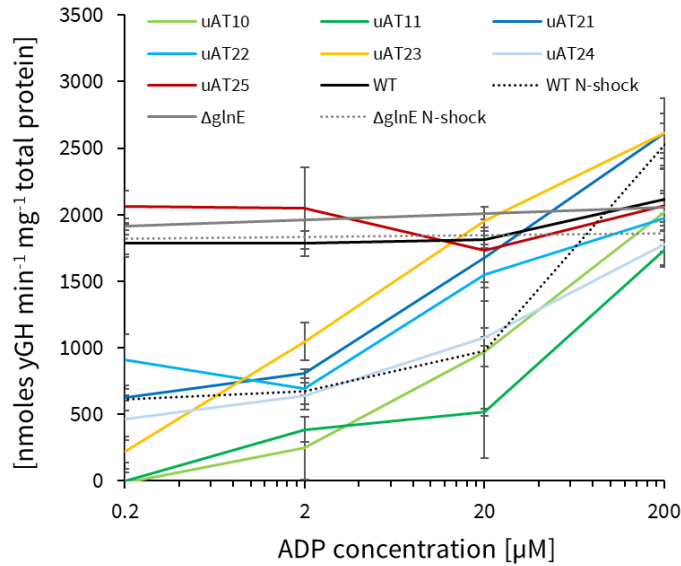
defined as the standard. FI denotes fluorescence intensity, EV denotes empty vector control, X denotes the circuit to be characterized. Error bars are standard deviations of n=4 biological replicates. See [Fig S21] for genetic circuit diagrams and part sequences.

Figure S3: Glutamine synthetase (GS) activity measurements.



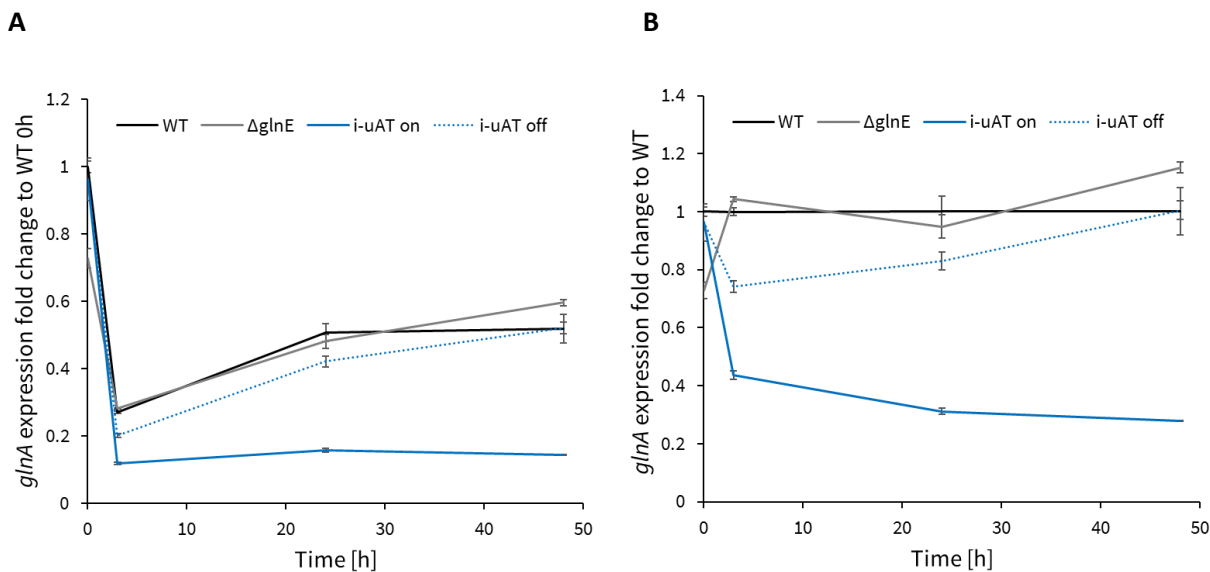
[A] Biosynthetic GS activity and quasi-reverse reaction of the γ -glutamyl hydroxamate assay. [B] Schematic of γ -glutamyl hydroxamate (γ GH) assay to determine glutamine synthetase activity of permeabilized whole cells. [C] Conversion of glutamine synthetase activities determined by the γ -glutamyl hydroxamate assay to adenylylation state.

Figure S4: Average glutamine synthetase (GS) activity measured by γ -glutamyl hydroxamate (γ GH) production at multiple ADP concentrations.



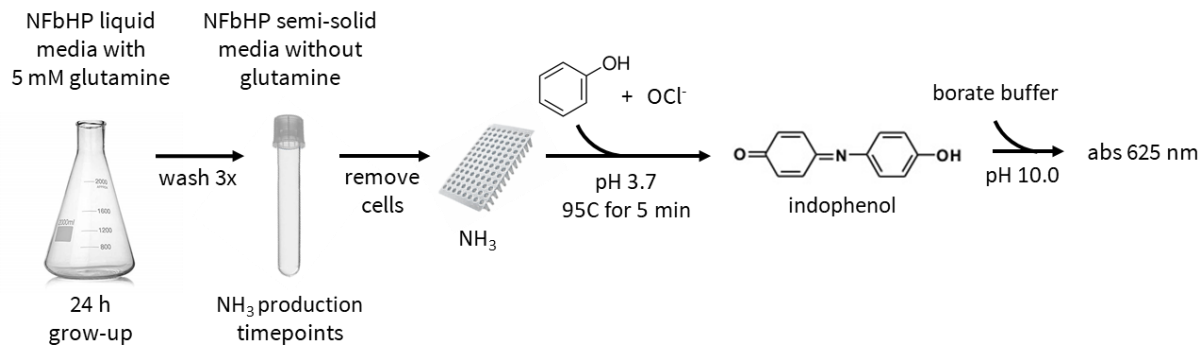
Constitutively unidirectional adenylyltransferases (uAT) expressing *A. brasiliense* $\Delta glnE$ strains [circuit R2 from pTS7, see Fig S21] were inoculated at OD₆₀₀ of 0.1 in semisolid NFbHP media and cells were processed as in [Fig S3B]. Rates were taken between 5 and 10 min timepoints and are normalized to total protein content determined by the Bradford assay. Wild-type (WT) and $\Delta glnE$ controls are not expressing uATs. Error bars are standard deviations of n=4 technical replicates. The N-shock controls show GS native adenylylation behavior after a 30 mM ammonium chloride shock 30 minutes prior to cell permeabilization.

Figure S5: Effect of uAT expression on *glnA* transcription under nitrogen fixing conditions.



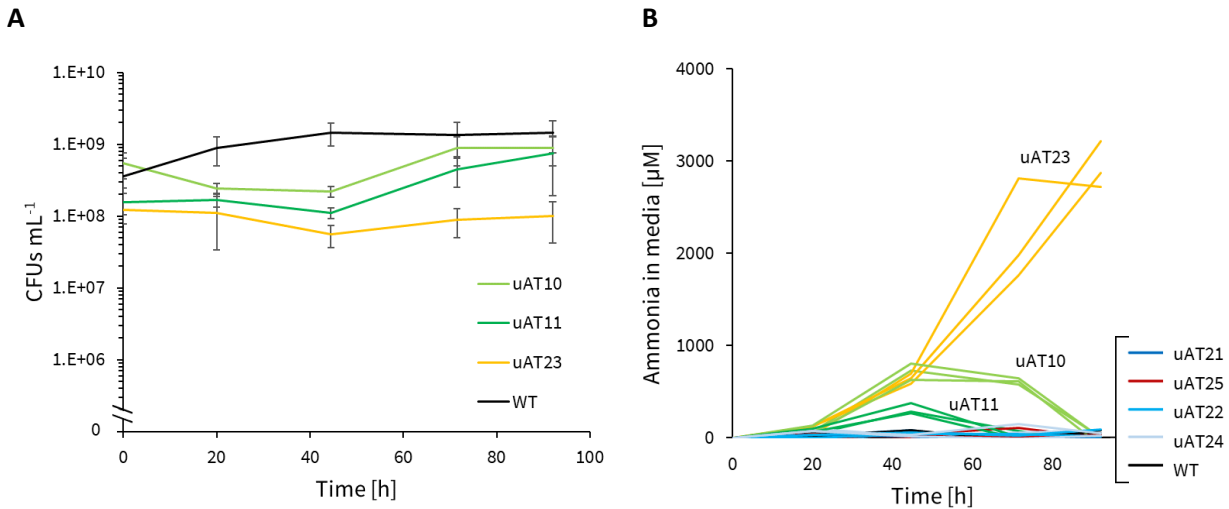
Reverse transcription quantitative polymerase chain reaction (RT-qPCR) analysis of *glnA* transcription levels in *A. brasiliense* wild-type (WT), $\Delta glnE$, and $\Delta glnE$ expressing plasmid uAT10 from the inducible circuit J3 [Fig S21] in the on and off states. To establish nitrogen fixing conditions, cells were inoculated in semisolid NFbHP media at OD₆₀₀ 0.1 and the on-state cultures induced with 200 ng/mL anhydrotetracycline at 0 h; biological replicate tubes were setup such that one tube would be harvested and extracted for RNA at each timepoint. Error bars show technical triplicates by RT-qPCR. Fold changes in [A] are relative to WT at 0 h (immediately after grow-up in NFbHP with 5 mM glutamine), and relative to WT at each timepoint in [B]. Fold changes were computed using the Pfaffl method, incorporating primer efficiencies and *glyA* as a previously reported housekeeping control gene(13, 14).

Figure S6: Ammonia measurements.



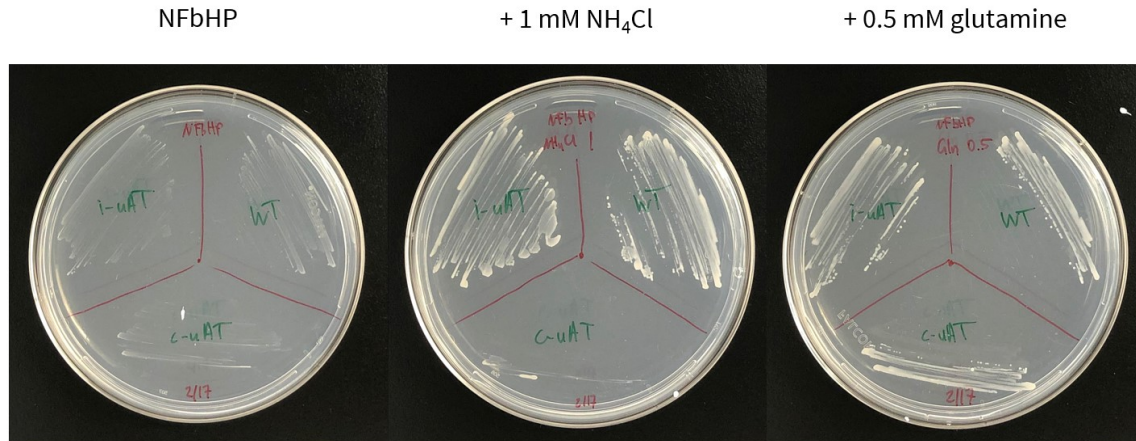
Schematic of indophenol assay to determine ammonia concentration in media.

Figure S7: Colony forming units (CFUs) of constitutive unidirectional adenylyltransferase (uAT) expressing *A. brasiliense* $\Delta glnE$ strains.



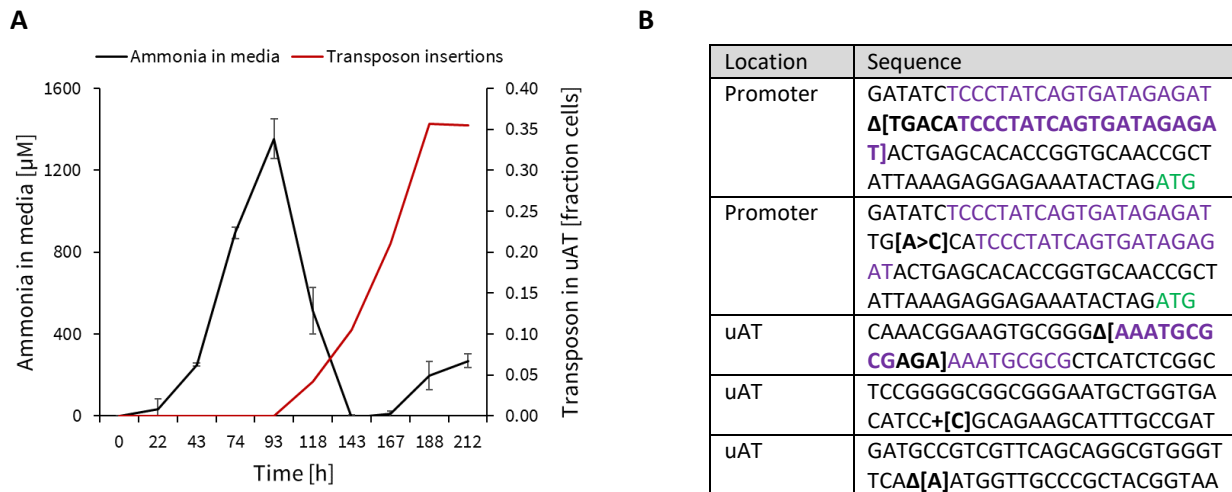
Strains were inoculated at OD_{600} of 0.1 in semisolid NFbHP media [circuit R2 from pTS7, see Fig S21]. **[A]** CFUs were counted from plating culture dilutions on LB agar plates. Error bars are standard deviations of biological triplicates. Ammonia in media is shown in Fig 2C and reproduced here in **[B]** for convenience to show the growth trade-off during ammonia production.

Figure S8: Role of supplemental glutamine on colony formation of uAT expressing strains grown on solid media.



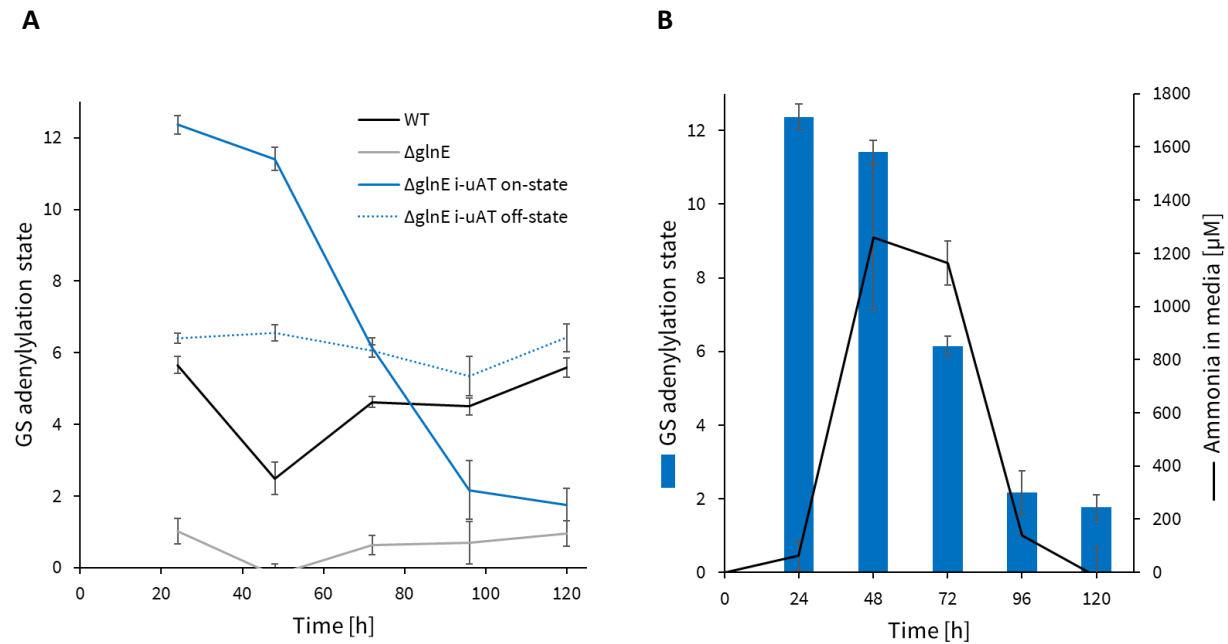
A. brasiliense wild-type (WT), $\Delta glnE$ constitutive uAT (c-uAT), and $\Delta glnE$ inducible uAT (i-uAT) expressing strains were plated on NFbHP media with either no added nitrogen source, 1 mM NH₄Cl or 0.5 mM glutamine. The glutamine concentration used was half that of NH₄Cl to keep the concentration of total nitrogen the same. uAT strains are stable chromosome integrations of c-uAT and i-uAT circuits [Fig S21] to allow for antibiotic free plating and growth comparison alongside WT. Plates were imaged after 2 days at 30°C.

Figure S9: Strain stability of ammonia production.



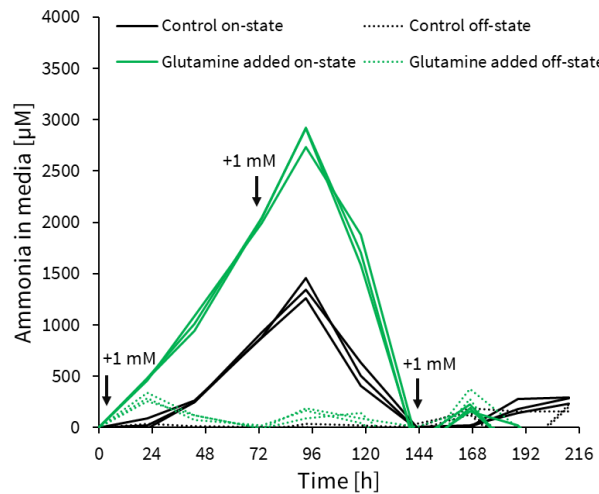
[A] Average time course data of ammonia in the media of *A. brasiliense* $\Delta glnE$ with inducible on-state (200 ng mL⁻¹ anhydrotetracycline) expression of uAT10 on circuit J3 from pTS7 [see Fig S21 for genetic circuit diagram and parts] inoculated and induced in semisolid NFbHP media at OD₆₀₀ of 0.1. Ammonia concentrations were determined by the indophenol assay; error bars are standard deviations of biological triplicates [see Fig S4 for assay]. Transposon insertions were quantified by plating cultures at timepoints, PCR amplifying the uAT cassette of individual colonies, and evaluating amplicon length on a DNA agarose gel. 8 colonies were screened per biological replicate culture per timepoint, their transposon insertions summed, and converted to a fraction estimating the total number of cells containing transposons in the uAT cassette at each time point. **[B]** Examples of other, non-transposon mutations found by sequencing; mutational sites have been bolded, repeats colored in purple, and start codons colored in green.

Figure S10: Glutamine synthetase adenylylation changes as ammonia is depleted over time.



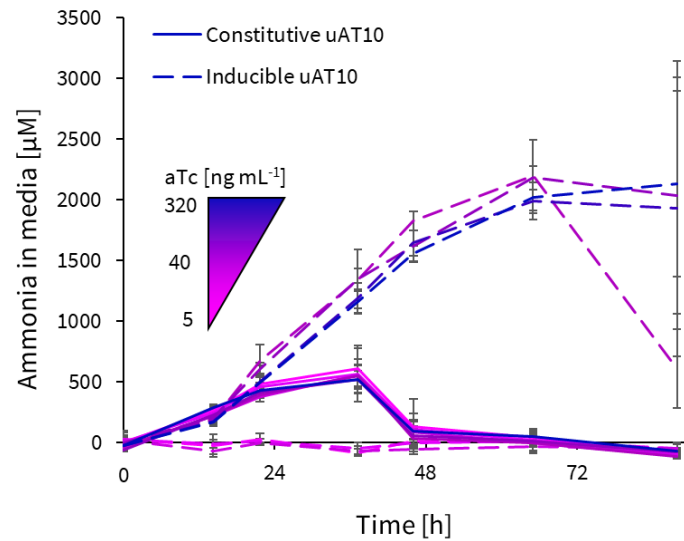
[A] Glutamine synthetase (GS) adenylylation state time-courses under nitrogen fixing conditions for *A. brasiliense* wild-type (WT), *glnE* knockout ($\Delta glnE$), and inducible uAT (i-uAT) expression in the $\Delta glnE$ strain either on-state or off-state. [B] Ammonia production time course in the i-uAT on-state cultures overlaid onto GS adenylylation. Cells were inoculated in semisolid NFbHP media at OD_{600} 0.1 and the on-state cultures induced with 200 ng/mL anhydrotetracycline at 0 h. The i-uAT in this experiment is pTS7 plasmid expressed uAT10 on circuit J3 [Fig S21]. Ammonia was quantified by the indophenol procedure [Fig S5] and GS adenylylation state by the γ -glutamyl hydroxamate assay [Fig S3]. All error-bars are standard deviations of technical triplicates.

Figure S11: Effect of the addition of exogenous glutamine on ammonia production.



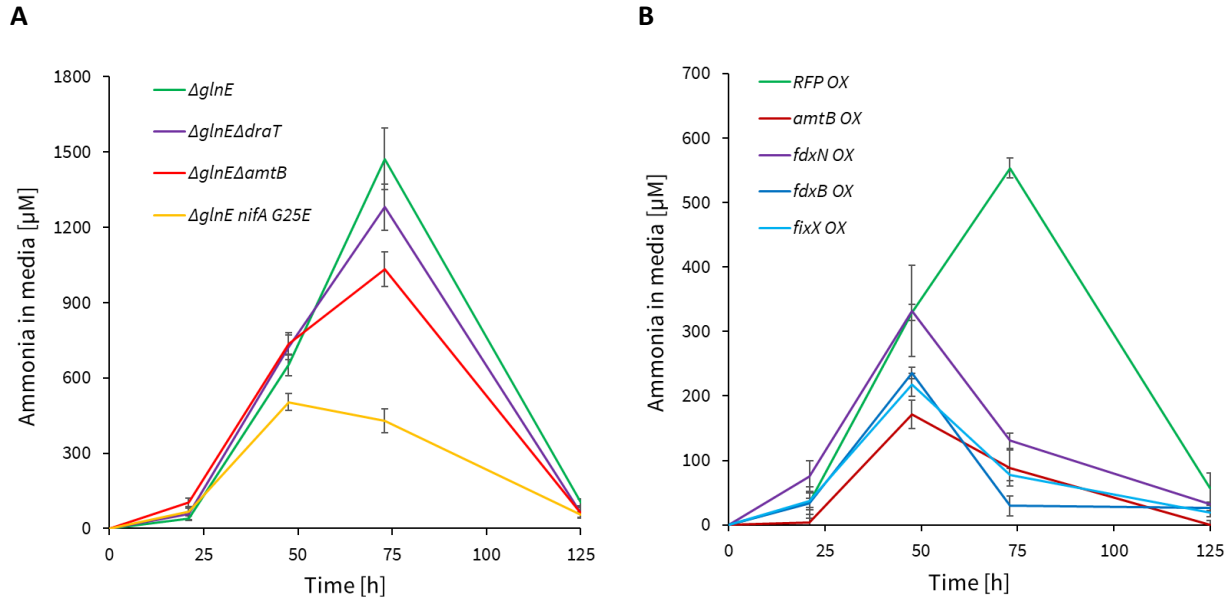
Ammonia production time-courses under nitrogen fixing conditions for *A. brasilense* $\Delta glnE$ expressing plasmid uAT10 from the inducible circuit J3 [Fig S21] with exogenous glutamine added to the media at indicated timepoints. Cells were inoculated in semisolid NFbHP media at OD_{600} 0.1 and the on-state cultures induced with 200 ng/mL anhydrotetracycline at 0 h. Ammonia was quantified by the indophenol procedure [Fig S6].

Figure S12: Ammonia production controlled inducibly.



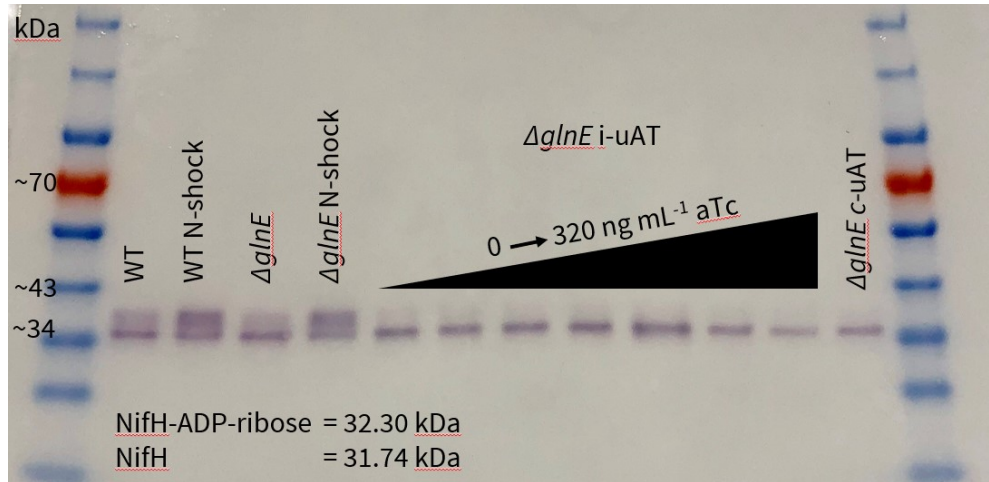
Average time course data of ammonia in the media of *A. brasiliense* Δ glnE with constitutive (circuit R2) and inducible (circuit J3) expression of uAT10 from pTS7 [see Fig S21 for genetic circuit diagrams and parts] inoculated and induced in semisolid NFbHP media at OD₆₀₀ of 0.1 at different anhydrotetracycline (aTc) inducer concentrations. Ammonia concentrations were determined by the indophenol assay; error bars are standard deviations of biological triplicates [see Fig S4 for assay].

Figure S13: Optimizing ammonia production through metabolic engineering.



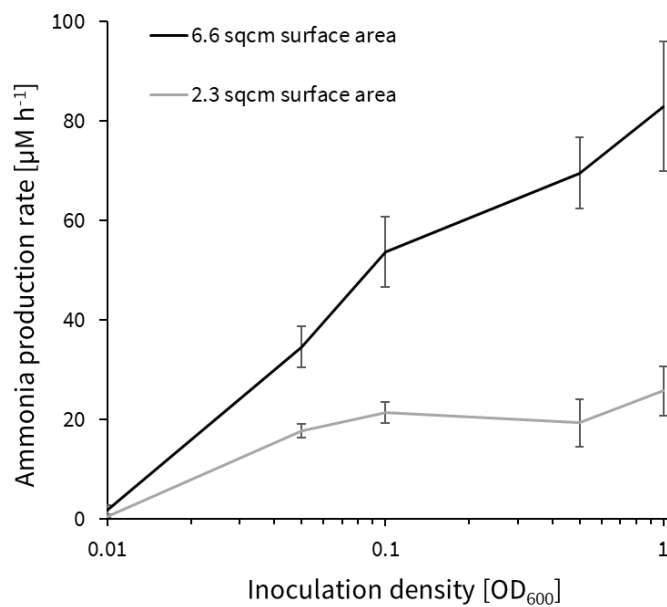
[A] For the knockout lines, native copies of *draT* and *amtB* were independently deleted in the *A. brasiliense* $\Delta glnE$ strain to generate double knockouts and the N-terminal region of *nifA* was mutated at G25E by double homologous recombination (15). In these strains, uAT10 was inducibly expressed on the J3 circuit from the pTS7 plasmid. Cells were inoculated in NFbHP at OD₆₀₀ of 0.1 and induced to on-state with 200 ng mL⁻¹ anhydrotetracycline. **[B]** For the overexpression (OX) lines, red fluorescent protein (RFP), *amtB*, *fdxN*, *fdxB*, and *fixX* were expressed as GOI2 on the OX3 circuit, with uAT10 being the first GOI [see Fig S21 for genetic circuit diagrams and parts]. Strains were assayed in the same way as in panel **[A]**. All ammonia concentrations were determined by the indophenol assay; error bars are standard deviations of biological triplicates [see Fig S4 for assay].

Figure S14: Effect of uAT expression on nitrogenase post-translational regulation.



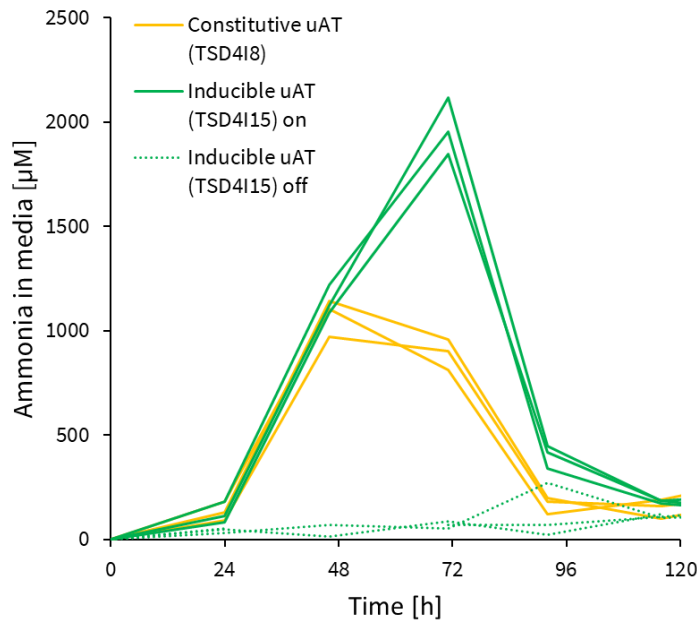
Nitrogenase activity is post-translationally deactivated by ADP-ribosylation through DraT and reactivated by hydrolysis of this post-translational modification though DraG [Fig S1]. Activation states of nitrogenase are shown above by Western blotting of nitrogenase subunit NifH in *A. brasilense* wild-type (WT), $\Delta glnE$, and $\Delta glnE$ stably expressing either constitutive uAT10 (c-uAT) or inducible uAT10 (i-uAT) across different anhydrotetracycline (aTc) inducer concentrations as indicated [Fig S21]. For this, cells were inoculated in semisolid NFbHP media at OD₆₀₀ 0.1 and induced as indicated at 0 h; cells were harvested at 24 h. Nitrogen shocks (N-shocks) denote addition of 20 mM NH₄Cl for 30 minutes prior to cell harvesting.

Figure S15: Gas diffusion limits ammonia production in semisolid media.



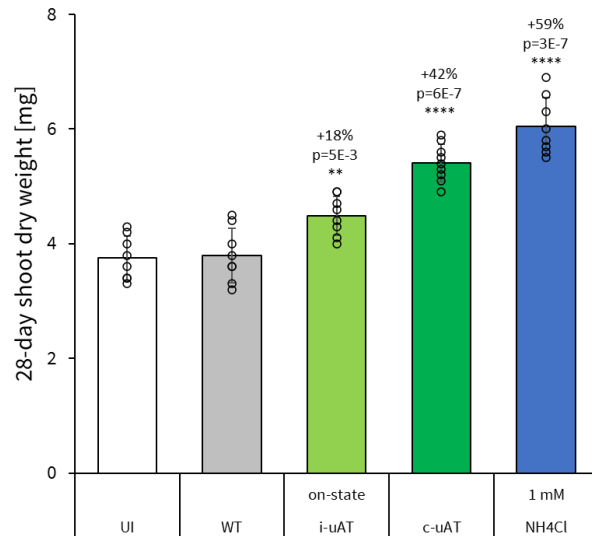
A. brasiliense $\Delta glnE$ transformed with pTS7 carrying inducible circuit J3 with GOI = uAT10 was inoculated and induced to on-state (200 ng mL⁻¹ anhydrotetracycline) at various ODs in 5 mL volumes in both 15 mL falcon tubes (surface area = 2.3 cm²) and 50 mL falcon tubes (surface area = 6.6 cm²). Average ammonia production rates were determined by the indophenol method between 24 and 48 h timepoints. Error bars are standard deviations of biological triplicates.

Figure S16: Chromosomally integrated uAT ammonia production.



Time course data of ammonia in the media of *A. brasiliense* $\Delta glnE$ stable lines for constitutive (TSD4I8) and inducible (TSD4I15) uAT10 unidirectional adenylyltransferases expression [see Fig S21 for genetic circuit diagrams, parts, and notes]. Strains were inoculated in semisolid NFbHP media at OD_{600} of 0.1 and on-state samples were induced with 200 ng mL⁻¹ anhydrotetracycline. Ammonia concentrations were determined by the indophenol assay [see Fig S4 for assay].

Figure S17: Effect of uAT expressing *A. brasiliense* Δ glnE strains on shoot dry weight of *S. viridis* in the absence of added sugar in the media.



A. brasiliense wild-type (WT) and Δ glnE strains with chromosomally integrated constitutive and inducible uAT10 circuits [Figs S16 and S21] were introduced at OD₆₀₀ 0.1 to 14 day old *S. viridis* plants growing gnotobiotically in modified 1/5 strength NFbHP with sodium lactate dropped out. At the time of inoculation, the i-uAT replicates were induced with 200 ng mL⁻¹ anhydrotetracycline. After an additional 14 days, shoot dry weights were collected. Percent growth promotion values are indicated above each bar and stars indicate p-values of statistical significance compared to WT using a two-sided homoscedastic t-test. All error bars are standard deviations of n=8-9 biological replicates.

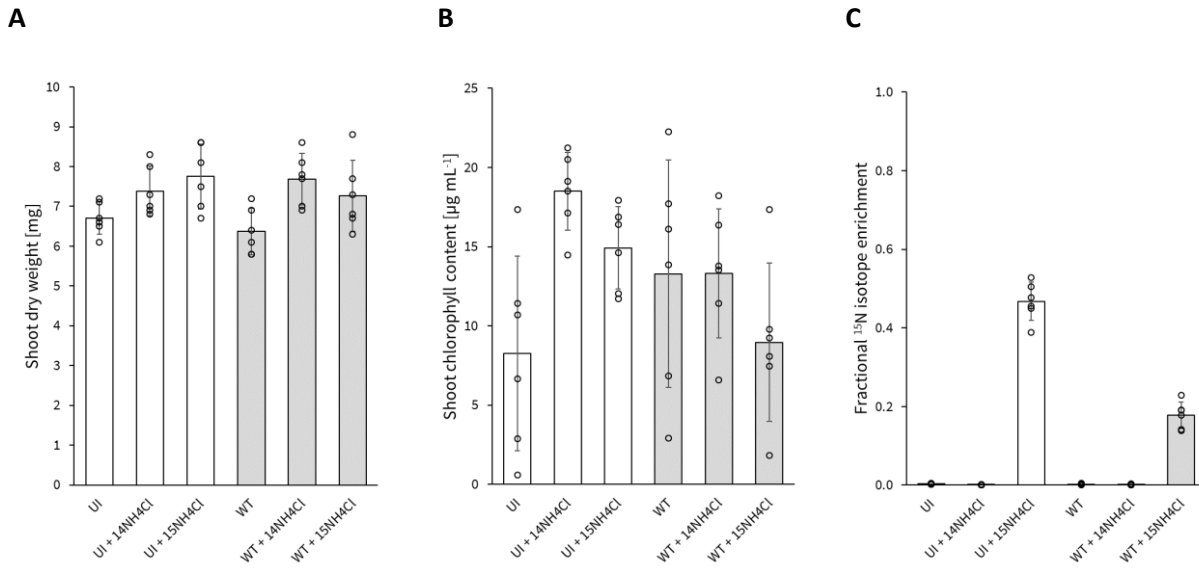
Figure S18: Calculation of fractional enrichment of ^{15}N isotopes in pheophytin.

$$\text{fractional } 15\text{N enrichment} = \frac{\langle \frac{m}{z} \rangle_X - \langle \frac{m}{z} \rangle_{STD}}{(number \text{ of } N \text{ atoms in molecule}) \cdot (15N \text{ neutron mass}) \cdot (maximal \text{ enrichment above nat. abundance})} \approx \frac{\langle \frac{m}{z} \rangle_X - \langle \frac{m}{z} \rangle_{STD}}{4 \cdot 0.997 \cdot 0.996}$$

where $\langle m/z \rangle = \sum_{isotopes} (\text{isotope mass} \cdot \text{relative abundance})$

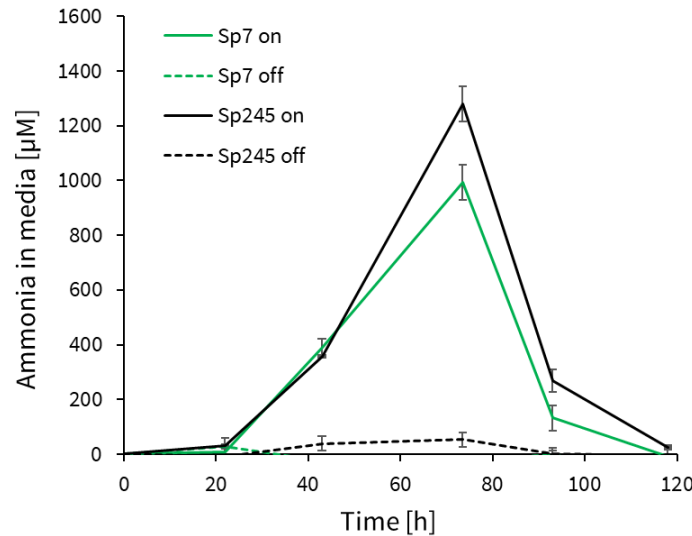
X denotes sample, STD denotes an authentic chlorophyll standard processed to pheophytin and assayed identically to samples of interest, and relative abundances have been normalized to 1. Calculation assumes natural abundance to be 0.4%.

Figure S19: Fertilized controls of *S. viridis* ^{15}N isotope integration either uninoculated (UI) or wild-type (WT) *A. brasiliense* inoculated.



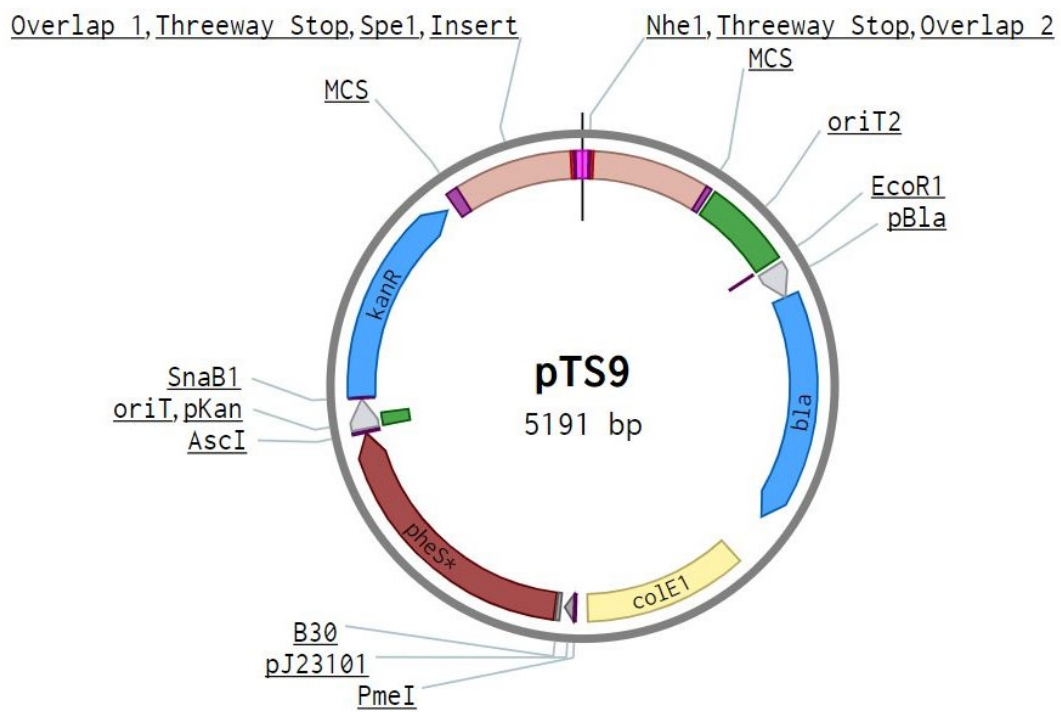
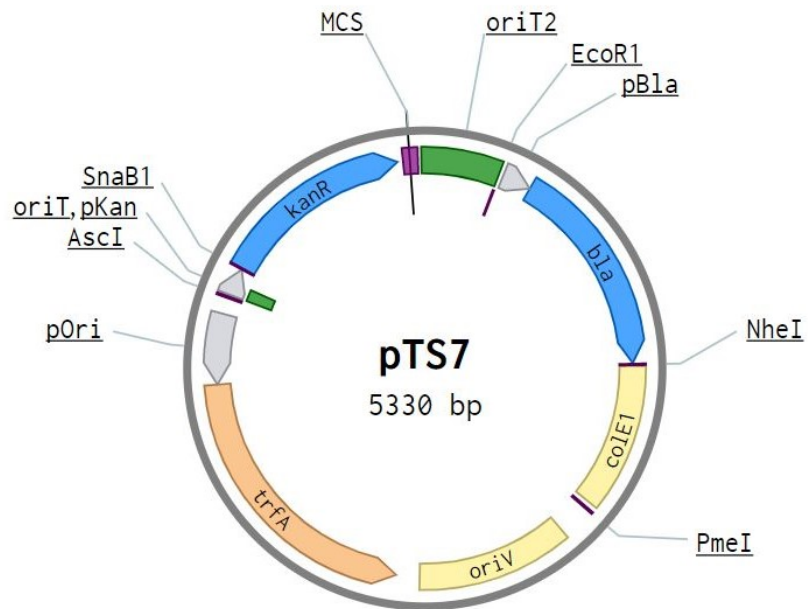
Ammonium chloride fertilizer was introduced at 1 mM and microbes were introduced at OD₆₀₀ 0.1 to 14 day old *S. viridis* plants growing gnotobiotically in modified 1/5 strength NFbHP at room atmosphere. At 14 days post inoculation, shoot dry weight [A] and total chlorophyll content [B] were collected. Chlorophyll was converted to pheophytin for isotopic analysis [C] to determine fractional enrichment of the ^{15}N isotope [see S12 for calculation]. All error bars are standard deviations of n=6 biological replicates.

Figure S20: Broad applicability of unidirectional adenylyltransferase (uAT) inducible ammonia production.



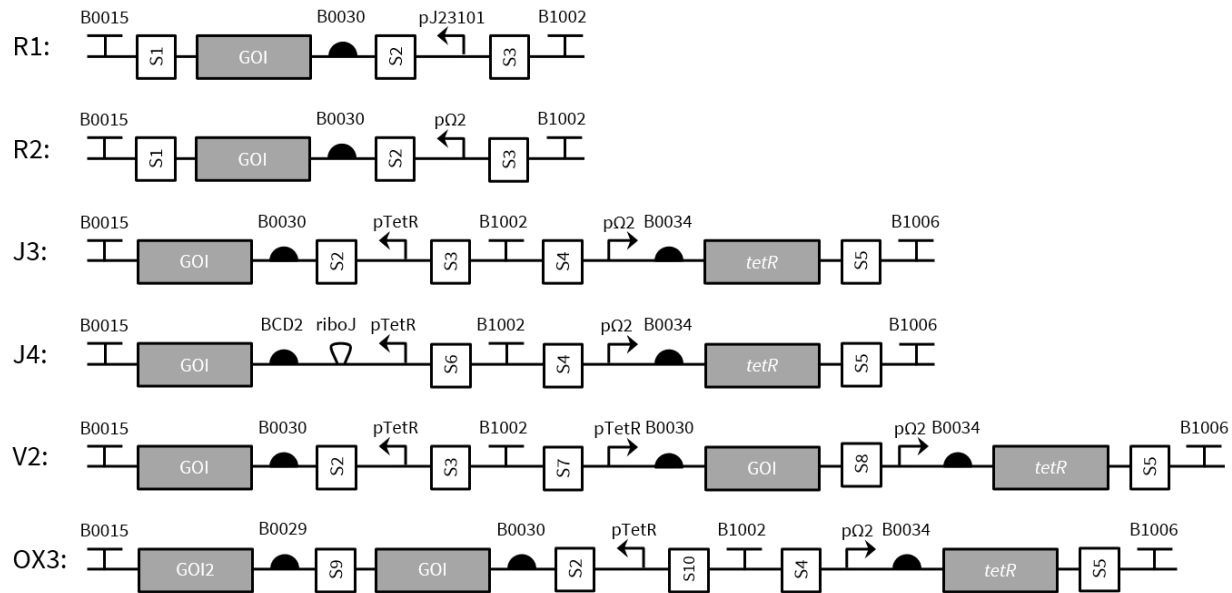
The native *glnE* of *A. brasiliense* Sp7 was disrupted and the J3 inducible circuit with uAT10 was inserted in a single step. This engineering was accomplished by single homologous recombination with a pTS7 plasmid that carried 1000 bp of *glnE* homology instead of *oriV* and *trfA*. The Sp245 control is the *A. brasiliense* Sp245 Δ*glnE* strain carrying the J3 inducible circuit with uAT10 on a plasmid. Strains were inoculated in semisolid NFbHP media at an OD₆₀₀ of 0.1 and on-state samples were induced with 200 ng mL⁻¹ anhydrotetracycline. Error bars are standard deviations of biological triplicates. [See Fig S21 for genetic circuits and parts].

Figure S21A: Plasmids designed for *A. brasiliense* used in this work.



The *oriV* broad host range origin for replication and kanamycin resistance were used for positive selection on our replicative plasmids (pTS7), while our integrative plasmids carried a negative selection marker and 0.5-1.0 kb homologous genomic regions instead of *oriV* for chromosome editing (pTS9). We find *pheS** to be highly effective as a negative selection maker in *A. brasiliense*, compared to other standard markers such as *sacB* (16). Overlaps 1 and 2 of pTS9 are 500-1000 bp of chromosome upstream and downstream of loci of interest; insert is the sequence to add or replace between homologous regions. Genetic circuit inserted into either plasmid are shown in [Fig S21B] and part sequences are shown in [Fig S21C]. Sequences of these plasmids have been deposited at GenBank with accession numbers MW835297 for pTS7 and MW835298 for pTS9.

Figure S21B: Genetic circuit diagrams.



Abbreviations are as follows, genes of interest (GOI): red fluorescent protein (RFP) for circuit testing or unidirectional adenylyltransferase (uAT) for ammonia production. Circuits R1 and R2 are for constitutive expression, J3 and J4 are for inducible expression. RFP data of these circuits is shown in [Figs S2A-B]. Circuit V2 contains a second copy of GOI for increased evolutionary stability (recommended to be codon refactored) [Fig 3C], while circuit OX3 contains polycistronic GOI2 for overexpression of an additional gene of interest, such as *amtB*, *fdxB*, *fdxN*, or *fixX* [Fig S13B]. All part sequences are shown and annotated in [Fig S21C]. Sequences of these circuits have been deposited at GenBank with accession numbers MW835306-MW835311 in the order they are shown above; GOI place holders for these submissions are as follows: GOI=RFP for circuits R1 and R2; GOI=uAT10 for circuits J3, J4, V2, and OX3; GOI2=RFP for circuit OX3.

Figure S21C: Sequences of genetic parts used in plasmids [Fig S21A] and circuits [Fig S21B]. All part sequences below are shown in their forward direction as depicted in [Fig S21B]; promoter, ribosome binding site (RBS), terminator, and spacer directions correspond to the genes they are flanking. Note: RBSs are separated 6 bp from gene start codons - those spacers are not shown. Parts named BBa are from the BioBrick Registry of Standard Biology Parts; other part sources are either described if common, or referenced if specific. GenBank accession numbers are shown for deposited sequences (all uATs).

Name	Notes	Sequence
<i>colE1</i>	Origin of replication from pUC19	TTGAGATCTTCTTCGCGCTAAATCTGCTGCTTGCACAAACAAAAACCACCGCTACCAGCGGTGGTTTG TTGCCGGATCAAGAGCTACCAACTCTTTCCGAAGGTAACTGGCTTCAGCAGAGCGCAGATAACCAAATA CTGTTCTCTAGTGTAGCGCTAGTTAGGCCACCACTCAAGAACACTGTAGCACGCCCTACATACTCGCTC TGCTAATCTGTACCATGGCTGCTCCAGTGGCATAAGTCGTGCTTACCGGTTGACTCAAGACGA TAGTTACCGATAAGGCGCAGCGTGGGCTGAACGGGGGGTCTGTGACACAGCCAGCTGGAGCGA ACGACCTACACCGAAGTACCTACAGCGTAGCTATGAGAAAGCGCACGCTCCGAAGGGAGA AAGGGGACAGGTATCCGTAAGCGCAGGGTGGAAAGGGAGAGCGCAGGAGGGAGCTTCAGGGG GAAACGCCTGGTATCTTATAGTCCTGCGGGTTCTGCCACCTGACTTGAGCGTCGATTTGTATGCT CGTCAGGGGGCGGAGCCTATGGAAA
<i>oriV</i>	Origin of replication from pEAQ-HT (17)	CCGGGAGGGTTCGAGAAGGGGGGACCCCCCTCGCGCTGCGCGGTACCGCAGGGCGCAGGCC TGGTTAAAACAAGGTTATAAATATTGGTTAAAGCAGGTTAAAGACAGGTTAGCGGTTGGCGAAA ACGGCGAAACCCCTGCAATGTTCTGCCTGTGGACAGCCCTCAATGTCATAGGTGCGC CCCTCATCTGTCACTGCCCCCTCAAGTGTCAAGGATCGCCCCCTCATCTGTCACTGAGTCGCGCCCT CAAGTGTCAATACCGCAGGGCACTTATCCCAGGCTGTCCACATCATCTGTGAAAACCTCGCGTAAAC AGGGCTTCGCGCAGTTGCGAGGCTGGCAGGCTCCACGTCCACGTCGCGCCGGCAGAACATCGAGCTGCCCC GTCAACGCCGCCGGGTGAGTCGGCCCTCAAGTCAACGTCGCCCTCATCTGTCACTGAGGGCCA AGTTTCCGCGAGGTATCCACAACGCCGCCGGCCGGTGTCTGCACACGGCTTCGACAGGGCTTCTGG CGCGTTGCGGCCATAGCGGCCAGGCCAGCGGAGGGCAACCAGCGCG
<i>trfA</i>	Required for <i>oriV</i> , also from pEAQ-HT (17)	ATGAATCGGACGTTGACCGGAAGGCATAACAGGAAGAACATGATCGACGCGGGTTTCCGCCAGGAT GCCGAACCATCGCAAGCGCACCGTATCGTGTGCGCCCGCGAACCTTCAGTCGCTCGATGG TCCAGCAAGCTACGGCAAGATCGAGCGCGACAGCGTCAACTGGCTCCCTGCCGCCCCGCCATC GGCCGCCGTGGAGCGTTCACGTGTCTCGAACAGGAGGCGCAGGTTGGCGAAGTCGATGACCATCGA CACCGAGGAACATGACGACCAAGAACAGCGAAAACCGCCGGCAGGACCTGGAAACAGGTAGCG AGGCCAACGAGGCCGTTGCTGAAACACACGAAGCAGCAGATCAAGGAATGCAAGCTTCTTGTGCA TATTGCGCGTGGCCGGACAGATCGAGCGATGCCAACGACACGCCGCTCTGCCCTGTTACCAAC CGCAACAAGAAAATCCCGCGAGGCAGCTGCAAACAAAGGTATTTCCACGTCACAAAGGACGTGAAG ATCACCTACCCGGCTCGAGCTGCGGGCGACGATGCGAACACTGGTGTGCCAGCAGGTGTTGGAGTAC GCGAACGCGCACCCCTATCGCGAGCGATCACCTCACGTTACGAGCTTGCAGGACCTGGCTGGT CGATCAATGGCCGGTATTACACGAAGGCCGAGGAATGCCGTGCGCCCTACAGGCCAGGGATGGGCT TCACGTCGCCACCGCGTGGGGCACCTGGAATCGGTGTGCGCTGCTGACCGCTCCCGCTCTGGACCGTGG CAAGAAAACGTCGGTGCAGGCTGATCGACGAGGAATCTGCGTGTGCTTGTGGCAGGACCACT ACGAATTATGGGAGAAGTACCGCAAGCTGCGCCAGGCCGACGGATGTTGCACTATTCAGCT CGCACGGGAGCGTACCCGCTCAAGCTGAAACCTTCCGCTCATGTCGGATGGATTCAACCGCGT GAAGAAAGTGGCGCGAGCAGGTGGCGAAGCTGCGAAGGTTGCGAGGAGCGGGCTGGTGGAACACG CCTGGGTCATGATGACCTGGTGCATTGCAAACGCTAG
<i>oriT</i>	Origin of transfer (also functions as a promoter and is part of pKan) from pBBR1	GGTCACGACTTGCAGAACAGTACTGAGTATACTCAAGCATTGAGTGG

riboJ	Previously reported for reliable gene expression (19)	AGCTGTCACCGGATGTGTTCCGGTCTGATGAGTCGTGAGGACGAAACAGCCTACAAATAATTGT TTAA
B0029	BBa_B0029	TTCACACAGGAAACC
B0030	BBa_B0030	ATTAAGAGGGAGAAA
B0034	BBa_B0034	AAAGAGGGAGAAA
BCD2	Previously reported for reliable gene expression (20)	GGGCCCAAGTTCACTAAAAAGGAGATCAACAATGAAAGCAATTTCGTACTGAAACATGTTAACCATGCT AAGGAGGTTTCTA
B1002	BBa_B1002	CGCAAAAACCCCGCTTCGGCGGGGTTTTTGC
B1006	BBa_B1006	AAAAAAAAACCCCGCCCTGACAGGGCGGGTTTTTT
B0015	BBa_B0015	CCAGGCATCAAATAAAACGAAAGGCTAGTCGAAAGACTGGGCCTTCGTTTATCTGTTGTTGCGGTG AACGCTCTACTAGACTGGCTCACCTCGGGTGGGCCTTCTGCGTTATA
Threeway stop	Stop codons frameshifted to stop every ORF (this work)	TAGCTAACTGA
S1	Spacer (this work)	TCGAAGTACTAGTTAGATGATAGGAT
S2	Spacer (this work)	ACCGGTGCAACCGCT
S3	Spacer (this work)	CGCAGGAGCTAGGCAGCGCTCACGATATC
S4	Spacer (this work)	GCGACCTGCGTCGCTAGAGCGAG
S5	Spacer (this work)	TAGTAGGCTAGAAACCTAGATGATGATT
S6	Spacer (this work)	CGCAGGAGCTAGGCAGCGCTCACGATATCTTCAGCAGGACGCACTGACC
S7	Spacer (this work)	GCGACCTGGGTCTATGTTGGGTTGACATC
S8	Spacer (this work)	CACGTGGCGTCGCTAGAGCGAG
S9	Spacer (this work)	CAATTGACATGAGTTACTGGCCCTGATTCTCCGCTTAAATACCGCACA
S10	Spacer (this work)	CGCAGGAGCTAGGCAGCGCTCACGATATCTCCCTACAGTGATAGAGATTGACA
uAT10	E. coli glnE 423-946, similar to AT-C 425-946 (2)	ATGGCACATATGACCAATGTGCGCCGGTGTAAATGAATTGATGGCAGATGAAAGTGAACACTCAGG AAGAGTCGCTGCGAACAGTGGCGTGAGCTGTCGAGGATGCGTTGAGGAAGATGACACTACGCCAG TGCTGGCGCATTTAGCGAGGATGATCGCAAACAGGTGCTAACGCTGATTGCCATTCCGCAAAGAGCT GGATAAGCGCACCATCGGGCGCGAGGACGTCAGGTGCTGACCATCTGATGCCCATCTGCTAAGTGT GTCTGTGGCGTGAAAGACGCTGCCATTACGCCCTGCTGGTGGGGATTGTTACCC GCACCACTATTAGAATTGCTAGTGAATTCCCGCGCGCTAAACATTGATTTCTGTCGCGCT CGCCGATGATTGCCAGCCAGCTGGCGCTTACCGCAGTGGTGCAGTTGCGCAGTATTGCTGCGATCAAACACCC TACCAAGCCGACGGCGACCGATGCCCTACCGCGATGAGTTGCGCAGTATTGCTGCGCTGCCGGAAAGATG

	Accession: MW835299	ACGAAGAGCAACAGCTTGAGGCCTGCGTCAGTTAACACAGGCGCAGCTTACGCATGCCGCAGCGG ATATCGCCGGTACGCTACCGGTATGAAAGTGAAGCGATCACTTAACCTGGCTGGCGGAAGCCATGATAGA TGCCGTCGTTACGCAGGGCTGGGTTCAAATGGTGCCTACGGTAAGCCGAATCACCTGAACGAACGC GAAGGGCGTGGTTTGCCTGGCTGGCTACGGCAAGCTGGCGGCTGGGAGTTAGGCTACAGTCCGAT CTTGACCTTATCTCCCATGATGCCAATGGATGCGATGACTGACGGTGAACGGGAAATCGACGGG GGCAGTTTATCTCGCTGGCGCAACGCATTATGCATCTGTTAGCTACGGTACCTCTCCGGCATTTG ATGAAGTGGATGCTGACTCGTCCTCGGGCGGGGAATGCTGGTACATCCGCAGAACGATTG CCGATTATCAGAAAACGAGGCTGGAGCTGGGAACATCAGGCCTGGTGCCTGAGTGTACG GCGATCCGCAACGGCAGTGCCTGGCGACTTGAACGCGAGTGGCTGGGAGATTATGACGCTGCCGTGAAGGTA AACTCTGCAAACGGAAGTGCAGGGAAATGCGCAGAAAATGCGCCTCATCGGCAATAAACATCGCA TCGTTGATATCAAAGCTGATGAAGGGGAATTACCGATATCGAATTATTACCAATATCTGGTGTGC GCTACGCTCATGAAAACGAGTAAACGCGTGGTACAGAACGCTGCTATTCTGAAACTACTGGCGA AAACGACATTAGGAAGAGCAGGAAGCGATGGCCTGACCCGTGTTACACTACGCTTCGCGATGAACCT CATCATCTGCATTACAGAATTGCCGGCATGTGCGAGGATTGCTTACCGCAGAGCGTGAACCTGG TGCAGCTGGCAGAAGTGGCTGGGAAGAATGA
uAT11	<i>E. coli</i> <i>glnE</i> , 609-946 (3)	ATGGACGAAGAGCAACAGCTTGAGGCCTGCGTCAGTTAACACAGGCGCAGCTTACGCATGCCGC GCGGATATCGCCGGTACGCTACCGGTATGAAAGTGAAGCGATCACTTAACCTGGCTGGCGGAAGCCATG ATAGATGCGCTGCTTACGAGGGCTGGGTTCAAATGGTGCCTACGGTAAGCCGAATCACCTGAACG AACCGAAAGGGGGCTGGTTGGCGTGGCGTACGGCAAGCTGGGGCTGGGAGTTAGGCTACAGT CCGATCTGACCTTATCTCCCATGATGCCAATGGATGCGATGACTGACGGTGAACGGGAAATCGAC GGCGCGCAGTTTATCTCGCTGGCGCAACGCATTATGCATCTGTTAGCTACGCTACCTCTCCGGCAT TTGTATGAAGTGGATGCTGACTCGCTCCGGCGGGGAATGCTGGTACATCCGCAGAACG ATTGCCGATTATCAGAAAACGAGGCTGGAGCTGGGAACATCAGGCCTGGTGCCTGCGTGTAGT GTACGGCGATCCGCAACGGCAGTGCCTGGCGCAGTTGACGCACTGCGTGCAGGAGATTATGACGCTGCCGTGA GGTAAAACCTCTGCAAACGAGTGCAGGGAAATGCGCAGAAAATGCGCCTCATCGGCAATAAACAT CGCGATCGCTTGATATCAAAGCTGATGAAGGGGAATTACCGATATCGAATTATTACCAATATCTGGT GTTGCGCTACGCTCATGAAAACGAGTAAACGCGTGGTACAGAACGCTGCTATTCTGAAACTACTG GCGAAACGACATTATGGAAGAGCAGGAAGCGATGGCCTGACCCGTGTTACACTACGCTTCGCGAT GAACCTCATCTGCATTACAGGAATTGCCGGCATGTGCGAGGATTGCTTACCGCAGAGCGT AACTGGTGCAGGGCAAGCTGGCAGAAGTGGCTGGTGAAGAATGA
	Accession: MW835300	ATGCTCGCCGGTGGAGGAGGCTACGCCAGCTTCGAGGGAGGCCGCGCTGCTGTCCGGCCCCGGC AACCTGCTTCACCGGACCGACGAGCCCCGGCACGGTGAAGACGCTGGCGCATGGCTACCGC GACCCAGGGGGCTCATGCCGTTGGCTTACCGTGCACGGGGCTACGGTGAACGAGCTGGCAAGACCCC GGCGCGGGAGCTGCTGACCGAGCTGGTGCCTGGCGCATGGCTACGGTGAACGAGCTGGCAAG ACGACGCGCTGGTAAGTTCGACAGCTTCTGGAGCGGCTCCGGGGGGTGGCTTCTGCTT CATGCCAACCCCTGGCTGCTGCCCTGGTGCAGCGGGAGATCATGGCACGGCGCAGCTGGCGAGAC GTTGCGCAACCGCTGCGTCTGACGCGCTGCTGCGCAGCTGGCGAGATCATGGCACGGCG GGGGGCTGACGCCGGAGTACCGCGCTTACCGCGGGGCGACAACCTCGAGGATGCTGACCC GCGCGCTGGACCAACGACCAGCGCTCCGCCGGGGCGCACATCCTGCGCGCATACCGACGGCG CCGCTGCGCCCTTCTCGCGATCTGGCGACGTGGTGGTGCAGGGAGCTGGCCGCCGCGTGGAGGA GGAGTTGCCGCCGCCACGGCGCATCCCGCGCGCTGGTGGTGGCGATGGCAAGCTAGG CAGCGCGAGCTACCATCACCTCGACATCGACCTGATGTTGCTACGAGGTGCCGGGGCACCGC CAGTCGGACGGAGCCAAGCCGCTGGCCCCAACGAGTATTACATCAAGCTGACCGAGCGCTG CCATCACCCCGCGATGGCGACGGGGCTGTACGAGGTGGACATGCCGCTGCCGTGGCAAG CCGGTCCGCTGCCGACCGCGCTGGACCGCTTACCGCGTACAGGCCAAGGATGCCGCTGGAGGA CATGGCCCTGACCCGCCGCGCTCATGCCGATGTTCCGGCGGCGATCCGGCGCTGGCT GTCGAGTCGGCGATCCGGTGTGCTACCGGGCCGCGACCCGGCAAGGTGCTGCCGGACCTGCG GACATGCCGCCGCGATCGACAAGGAGTTCGGCACCAACCGTGGAACGTCAAA ACGCCGCCGG GGCCTGATCGACATCGAGTTACGGCCCTGCTCAACGCCGCTGCCGGCTGCTGCCGCCGGAG GTCCATGCCACCAGGCCGCCCTGCTCAACGCCGCTGCCGGCTGCTGCCGCCGGAG GGAGCTGGTGGCGACGCTGAAGCTGTTGGCGGGCTGAGGGCTCTGCCGCTGACCC GCGAGGAG GCTCGATCCGGCGAGGTTGCCAACCTGCCGGGGCTCTGCCGCGCCCTCCGGACGAGGAG CCGGCGGTTGACTTCGCCGCGCTGACAGCAGAACTCGGGACATCGGCCGCCGCCACGCCATT TGGCGTGGTCGAGGAGCCGGCTCAAGGCTGCCCTCCCGAGAGACCAACGAAGAAGCCAA CTCCATGA
uAT21	<i>A. brasiliense</i> <i>glnE</i> 449-1003 homologous to uAT10 (this work)	ATGCTCGCCGGTGGAGGAGGCTACGCCAGCTTCGAGGGAGGCCGCGCTGCTGTCCGGCCCCGGC AACCTGCTTCACCGGACCGACGAGCCCCGGCACGGTGAAGACGCTGGCGCATGGCTACCGC GCGCGGGGGAGCTGCTGACCGAGCTGGTGCCTGGCGCATGGCTACGGCTCCACCG GGCGCGGGAGCTGCTGACCGAGCTGGTGCCTGGCGCATGGCTACGGCTGGCG ACGACGCGCTGGTAAGTTCGACAGCTTCTGGAGCGGCTCCGGGGGGTGGCTTCTGCTT CATGCCAACCCCTGGCTGCTGCCCTGGTGCAGCGGGAGATCATGGCACGGCGCAGCTGGCGAGAC GTTGCGCAACCGCTGCGTCTGACGCGCTGCTGCGCAGCTGGCGAGATCATGGCACGGCG GGGGGCTGACGCCGGAGTACCGCGCTTACCGCGGGGCGACAACCTCGAGGATGCTGACCC GCGCGCTGGACCAACGACCAGCGCTCCGCCGGGGCGCACATCCTGCGCGCATACCGACGGCG CCGCTGCGCCCTTCTCGCGATCTGGCGACGTGGTGGTGCAGGGAGCTGGCCGCCGCGTGGAGGA GGAGTTGCCGCCGCCACGGCGCATCCCGCGCGCTGGTGGTGGCGATGGCAAGCTAGG CAGCGCGAGCTACCATCACCTCGACATCGACCTGATGTTGCTACGAGGTGCCGGGGCACCGC CAGTCGGACGGAGCCAAGCCGCTGGCCCCAACGAGTATTACATCAAGCTGACCGAGCGCTG CCATCACCCCGCGATGGCGACGGGGCTGTACGAGGTGGACATGCCGCTGCCGTGGCAAG CCGGTCCGCTGCCGACCGCGCTGGACCGCTTACCGCGTACAGGCCAAGGATGCCGCTGGAGGA CATGGCCCTGACCCGCCGCGCTCATGCCGATGTTCCGGCGGCGATCCGGCGCTGGCT GTCGAGTCGGCGATCCGGTGTGCTACCGGGCCGCGACCCGGCAAGGTGCTGCCGGACCTGCG GACATGCCGCCGCGATCGACAAGGAGTTCGGCACCAACCGTGGAACGTCAAA ACGCCGCCGG GGCCTGATCGACATCGAGTTACGGCCCTGCTCAACGCCGCTGCCGGCTGCTGCCGCCGGAG GTCCATGCCACCAGGCCGCCCTGCTCAACGCCGCTGCCGGCTGCTGCCGCCGGAG GGAGCTGGTGGCGACGCTGAAGCTGTTGGCGGGGGCTGAGGGCTCTGCCGCTGACCC GCGAGGAG GCTCGATCCGGCGAGGTTGCCAACCTGCCGGGGCTCTGCCGCGCCCTCCGGACGAGGAG CCGGCGGTTGACTTCGCCGCGCTGACAGCAGAACTCGGGACATCGGCCGCCGCCACGCCATT TGGCGTGGTCGAGGAGCCGGCTCAAGGCTGCCCTCCCGAGAGACCAACGAAGAAGCCAA CTCCATGA
	Accession: MW835301	ATGCCGGCACGGTGAAGACGCTGGCGCATGGCTACCGCGACCCAGCGGGGTACGCCGTGGT TCCACCTGCAACCGCGGGCTACCGCTCCACCGCTGGGGCGCCGGGGAGCTGCTGACCGAGCT GTGCGGGCATGCTGAACGAGCTGGCGAAGACCCCCCGCCGGACAGCGCTGGTGAAGTTCG ACAGC TTCTGGAGCGGCTTCCGGCGGGGGCTGTTCTGCTGTTACGCCAACCCCTGGCTGCTGCCCT GGTCGCGGGAGATCATGGCACGGCGCCGAGCTGGCGAGACGCTGGCGACCC CGCCGTGCTGCCGACTTCTGCCACCGCTGCCGGAGCGCGGGGGCTGACGCCGGAGTAC CGCG TTATCGCCGGCGCACAACCTCGAGGATGCTGACCC TCCGCTGCCGGCTGCCGCCGGAG TCCGCCGGGGCGCACATCTGCCGGCATACGCCACGCCGACCGCTGCCGCCCTCC GCCGATCT GGCCGAGCTGGTGGTGCCTGGAGCTGGCGCCGCCGCTGGAGGGAG GTTGCCGCCGCCACGCC CCCCGGCGGCCCTGGGGGGTGGTGGCGATGGCGAAGCTAGGCGACGGCAGCT CATCGACCTGATCGTGGCTACGAGGTGCCGCCAGCGGACGGAAGCCAAGCGC CATCGACCTGATCGTGGCTACGAGGTGCCGCCAGCGGACGGAAGCCAAGCGC AGCTGGCGTGGC
uAT22	<i>A. brasiliense</i> <i>glnE</i> 481-1003 (this work)	ATGCCGGCACGGTGAAGACGCTGGCGCATGGCTACCGCGACCCAGCGGGGTACGCCGTGGT TCCACCTGCAACCGCGGGCTACCGCTCCACCGCTGGGGCGCCGGGGAGCTGCTGACCGAGCT GTGCGGGCATGCTGAACGAGCTGGCGAAGACCCCCCGCCGGACAGCGCTGGTGAAGTTCG ACAGC TTCTGGAGCGGCTTCCGGCGGGGGCTGTTCTGCTGTTACGCCAACCCCTGGCTGCTGCCCT GGTCGCGGGAGATCATGGCACGGCGCCGAGCTGGCGAGACGCTGGCGACCC CGCCGTGCTGCCGACTTCTGCCACCGCTGCCGGAGCGCGGGGGCTGACGCCGGAGTAC CGCG TTATCGCCGGCGCACAACCTCGAGGATGCTGACCC TCCGCTGCCGGCTGCCGCCGGAG TCCGCCGGGGCGCACATCTGCCGGCATACGCCACGCCGACCGCTGCCGCCCTCC GCCGATCT GGCCGAGCTGGTGGTGCCTGGAGCTGGCGCCGCCGCTGGAGGGAG GTTGCCGCCGCCACGCC CCCCGGCGGCCCTGGGGGGTGGTGGCGATGGCGAAGCTAGGCGACGGCAGCT CATCGACCTGATCGTGGCTACGAGGTGCCGCCAGCGGACGGAAGCCAAGCGC AGCTGGCGTGGC
	Accession: MW835302	

		TCCGTCACGGCACCGCATCGGACATCCTGTCCATGCCACCAGCCGCCCTGCTCAACGCCGCTGCGGCCGGCTGCTGGCGAGGAGCTGGTGGCGACGCTGAAGCTGTGGCGCGGGTGA GGGCTTCCCTGCGCTGACCAACCGACGGCGTCTCGATCCGCAGGTTTGCCCACCCCTGCAGGGAGGGCTCTCGCCGCTGACAGCAGAATCCGGGACATCGCCGCCGCCACCGCATTCTGCGCTGGTCAGGAGCCGGCTCAAGGCTGCCTCCCCAGAGACCAACGAAGAACCAAACCTCCATGA
RFP	BBa_E1010	ATGGCCAGCAGCGAAGACGTTCAAAGAGTTATCGCCTTAAGGTCGGATGGAAGGCAGCGTAAACGGTATGAATTGAGATCGAAGGAGAAGGTGAAGGGCGTCCCTATGAGGGCACGCAGACGGCTAAGCTC AAAGTGACGAAGGGTGGACCTCTGCCCTTGCTGGACATCCTGCGCCAGTTTCACTGAAACTCAGTTCCCGAAGGTTCAAGTGGGAACCGAGTGAACCTCGAGGACGGC AGGCGTATGTGAAGCAGTCCGGCGACATCCCTGATTATCTGAAACTCAGTTCCCGAAGGTTCAAGTGGGAACCGAGTGAACCTCGAGGACGGC GAATTCACTTATAAGGTCAAACTCGAGGGACCAACTCCCGTCACTGAGATGGCCGGTGTATGCAAGAAAAAGA CTATGGGTTGGGAGGCAAGCACCGAGCGTATGATCCGGAGGATGGAGCCCTAAGGGTGAAGATCAAGA TGCCTGAAAGCTGAAGGATGGGGCATTACGATCGGAGGTTAAACACCTATATGGCAAGAAC CAGTCAGCTCCGGCGCGTATAAGACGGATATTAGCTGGACATCACCAGTCATAACGAAGACTACAC CATCGTCAAGAACATACGAGCGCGCCGAAGGGCGGCATTCAACGGGTGCCTGA
tetR	BBa_R0040 with LVA tag removed and codon refactored for <i>A. brasiliense</i> codon usage	ATGTCGGCCCTGGACAAGAGTAAGGTCTTAAATTCTGCCCTTGAATTGTCGAACGAAGTCGGCATCGAGG GTTGACCAACCCCGGAAGCTGGCTCAGAACAGCTGGGTGTCGAACAGCCGACGTTGACTGGCATGTGAAGA ACAAGAGGGCGTTGCTCGATGCCCTGCCATGAAATGCTGATGCCACCATAGCATTCTGCTCC GAGGGTGAATCGTGGCAAGACTCTGCCGAACAATCTCCGCTGCCCTCTTGCC TGATGGCGCCAAGGTGCACTGGGCACCCGTCGACGGAAAAGCAGTATGAGACACTAGAGAACAGCT CGCTTCTCTGCCAACAGGGTTTAGCCTGAAAAGCCCTGATGCTGTTGTCGGGGTGGGACATTCA CTCTGGCTCGCTTGGAGGACAGGAGCATCAGTGGCGAAGGAAGAGCGTGAACCGGCAAC ATTCTATGCCGCCGCTGCTGCGGAGGGCATGAACTTTGACCAAGGAGCTGAACCGGCTTCT GTTGGTTGGAACTCATTATTGCGGTTGGAGAACAGCTTAAGTGCAGAACGGATCATGA
amtB	From the <i>A. brasiliense</i> genome	ATGAGCGCTCTTCACCCCTGCCGCCGACGATGGCGGCATTCTGGCTTGGCGCTGCTGCC CCGCCCTGCCGCCAGGAAGCGGCCGCCGCCGCCAGGCCAGCCCACCCCTGAGCAGCGGCACACGGCTTGA TGCTGGTCGCCACGGCGCTGGCTGTTCTGTTATGACCATCCGGCTCTGGCCCTGTTCTACGGCGCATGGTC CGCAAGATGAACGTGCTGGCTGATGCAAGAGCTCGCATCTGCGATCTGCTGGTCA TCTCGCCGGTTACAGCATCGCTTACCGAAGGCACCCGTTACCGGAGCAGTCTCGTCTCCAGATGACCT GCCGCATCACGCCGGCTGATCACCAGCGCTTCCGGACCGCATGAAAGTTCTCTCGATGCTGGT TCACGGGCTGTTGTCGATCGTCTACCGCCGATACCCACTGGGCTGGGCTGGGCGGGCTATCT GGCGGGTACGGCGTCTGATTACCGCCGGCACCGTGGTCA CATCAACGGGGCGTGGCGCT CGTCGCCGCCATCGTCTGGCAAGCGAAGGGTACCCGAACGAGAACCTCGCCCGACAACCTGGT CTCAGCCTGATCGGCGCTCGATGCTGGGCTGGCTGGCTTCAACCGGGTTCCGCCGTTGGCG CCGACGGCGTGCAGGCATGGCATGCTGTCACGAGATCGCCGCCACCGCCGATGCTGG GCTGGTCAAGTGGGCCACCAAGGGCAAGGCTCGGCTCGGATCATCTCCGGCCATGCCGGCTG GTCGCCATACCCCGGCCCTCGGCTCGGCTCGGCGACCCGCGCCCTGGTATCGGCTGGCCGGCT TGATCTGACTGGGGGCCACCGGCCATGTCGGCGCATCTGACGGACTCGCTGGACGCCCTCG CGTCACGGCGTGGCGCATCGTGGCGCATCTGACGGCGCTTCCGCCAGGAAGGCCATGCCGG TACCGCCGCCCTGGAAAGGCAACGTCGGCCAGATCTGGACGGTCTACGGCATCTGCCACCATC GCCTACTCGCGGCTGGCTCTCATCTGAAGGTATCGACGTGGTATGGGCCCTGTCGACGA GGACGTGAGCGCGACGGCTGGACCTCGCCCTGACGGCGAGACCATCCACTAA
fdxB	From the <i>A. brasiliense</i> genome	ATGGCTGAGTTCTGACCGGACCAACCCCGGCCGCTGGACGCCAAATTCTGTGGAAAGCATC GACCGAGAAGATGTGACCGCTGCCGCTGCTTCAAGGTCTGCCGCCGACGTGCTGGAGCTGATC GGCATCACCGAGGACGGCGACATCGTCGACGCCCTGACGAGGCCGAGAACAGGCTATGAGCGTC AAGAACGCCGCCATTGACCGCTGCGAAAGCTGCCAGGCTGCTGGCAAGGCTGTTCAAGAACCTGAC TGCCCCAGCGGCTGA
fdxN	From the <i>A. brasiliense</i> genome	ATGGCTTACAAGATCAAGGCTTCCGACTGCACCGCTGCCGCCCTGCGAGGCCAGTGCCCACAAACG CCATCAGCTTACAAGAAGGGCCCTACGCCATACGCCGACCTGTCACCGAGCTGCAAGGGCCAGTTCTC CAGCCCGCAATGCCCTCGGCTGCCACTGCTGCCAGGCTACGGCATCTGCCGGCT TGATCTGACTGGGGGCCACCGGCCATGTCGGCGCATCTGACGGCGCTTCCGCCAGGAAGGCCATGCCGG CGTCACGGCGTGGCGCATCGTGGCGCATCTGACGGCGCTTCCGCCAGGAAGGCCATGCCGG TACCGCCGCCCTGGAAAGGCAACGTCGGCCAGATCTGGACGGTCTACGGCATCTGCCACCATC GCCTACTCGCGGCTGGCTCTCATCTGAAGGTATCGACGTGGTATGGGCCCTGTCGACGA GGACGTGAGCGCGACGGCTGGACCTCGCCCTGACGGCGAGACCATCCACTAA
fixX	From the <i>A. brasiliense</i> genome	ATGAGCATCGTGGTCAAGATCGAAGAGAACGCTGTACCGAGAACCGCTACATCGTGGACGAGGCCGCC CACATCCAGATCCGCAACGACGCCGCTGCAAGTCCCTGCGAGTCCAGGCCGACCGCTGCTGCCGG CGGCCGCTACAGCAAGAACGAGACCCGAGCGTACGCCGAGCTGCCAGGCCACCGACGGCTGCC CCTGCCGCCGGCTGCCAGGACAAGGAAATATTCAAGTGGGACTACCCACGGGGCGTACGGCATCA GTTATAAGTTGGTGA

Figure S21D: Sequence of chromosome modifications reported in this work. Lowercase letters are 100 bp flanking genomic regions, and uppercase letters are inserted sequences. All sequences have been deposited at GenBank and accession numbers are shown.

	<p>CGCAGATAAAACTGCCGCCGTGATTCCCGCTACCGTCAGTCATGCATCCATTGGCAATCATGGAG GAAGATAAAGGTCAGATCGGAACTGTAGCTAACTCCAGCCGCCAGCTTGCCTAGCCGACCACCGCA AAACCACGCCCTCGCGTTCTCGCTTACCGTATTGGCTTACCGTAGCCGGCAACCATTGAACCCACGCC CTGAAACGACGGCATTCTATCATGGCTTCCGCCAGGTTAACAGTGCTGCCTGTTGAACGTACGCC TACCGCGATATCGCTCGGGCATCGTAACAGCTGCCTGTTGAACGTACGCC TTGCTCTCGTATCTCCGGCACGGCAGCAAATACTGGCGAACTCATCGGGTAGGCATCGGCC TCGGCTGGTAAAGGGTTGGATCGAGCAATTCCAGCAATAATGGATAACCGCCAGCTGGCTGG AATCATGGCGACGGCACACAGAGAAAATCAAATGTTAACGCGCGGGAAATTCACTGAGCAATT AAATAGGGTGGTGGGGTAACAATCCCACAGCAAGCGGTAAATGCGCGACAGCGTAACGGCAGCGT TCACCGCAGACAGACATCACTAGCAGATCGGCATCAGATGGTCGAGCACCTGACGTCTCGGCC TGGTGCCTTACAGCTTGCAGGAATCGCAACTAGCGTTAGCACCTGTTGCATCATCCTCGTA AGATGCCAGCACTGGCGTAGTGTATCTCTGCACAGCATCTGCCAGCTACGCCACTGGCGA CAGCGACTTCTGAGTTTCACTTCATCGGCCAATCAATTCAAACACCGGCCACATTGGTCA ATGTGCATCTAGTATTCTCTTTAATAGCGGTGACCGGTGCTCAGTATCTACTGATAGG GATGTCATCTACTGATAGGGAGATATCGTGGAGCGCTGCTAGCTCTGCCGGCGAAAAAACCC GCCGAAGCGGGGTTTGCCTGGCGACCTGCGTAGCGCCTAGCGAGGAACCGGAATTGCCAGCTGGCG TCCAACACAAATGCCCTGGCGTAGACATAAGCCTCTGGCTGTAGGCTGTAATGCAGGTAGCGA ACCCGTTGGTCAAAACCTTCGGGTATGGCATGATAGCGCCCGAAGAGAGCTAACATTGAGGTGAGT AGCTCACTTATTAGGACCCCCAGGCTTACACTTATGCTCCGGCTCGTATGTTGTGGAATTGCTA GAGAAAGAGGAGAAACTCGAGATGCTCGCTGGACAAGAGTAAGGTATTAATTGCTGGAAATTG TGAACGAAGTCGGCATCGAGGTTGACCGACCGTGGCTCAGAAGCTGGTGCACAGCGA CGTTGACTGGCATGTGAAGAACAAAGGGCGTTGCTCGATGCCATGAAATGCTCGATGCC CCATACGCATTCTGTCTTGGAGGGTGAATCGGCAAGACTTCTGCGGAACAATGCCAATCTTCC GCTCGCTCTTGTCCCACCGTGTGGCGCAAGGTGATCTGGCACCGTCCACGGAAAAGCAGTA TGAGACACTAGAGAACCGAGCTCGCTGCTGCAACAGGGTTTAGCCTGGAAAACGCCCTGTATGCGT TGTGGCGTGGGACATTCACTCTCGCTGCTGGAGGACAGGAGCATCAGGTGGCGAGGAAG AGCGTAAACCCAACGACCGATTATGCGCCGCTGTCGGCAGCGATGAAACTTCTGAC AGGAGCTGAACCGGCCTCTGTTGGAACTATTATGCGGTTGGAGAACAGCTTAAGTGC GAATCGGATCATGATAATAGTAGGCTAGAACCTAGATGATGATGATTAAAAAAAAACCCGCCCTGAC AGGGCGGGTTTTTGCGTGATACGACAGATGGTTGGCTAGCTGAGTAGGTAGGTTGgaccc ggggagcgccagctcgccgcggcggagacggccggctggccgcctgatgcattggccgaac cgcatccgcaacgcggaggaaaggccaccaccccccacccctggaggagtggaggagg aaggcgctgggacaaggccaccaccccccacccctggaggagtggaggaggccccgg cgtaacggcgga</p>
--	---

References cited in supplemental materials

1. M. De Zamaroczy, Structural homologues PII and Pz of Azospirillum brasilense provide intracellular signalling for selective regulation of various nitrogen-dependent functions. *Molecular Microbiology* **29**, 449-463 (1998).
2. R. Jaggi, W. C. van Heeswijk, H. V. Westerhoff, D. L. Ollis, S. G. Vasudevan, The two opposing activities of adenylyl transferase reside in distinct homologous domains, with intramolecular signal transduction. *Embo j* **16**, 5562-5571 (1997).
3. P. Jiang, A. A. Pioszak, A. J. Ninfa, Structure-function analysis of glutamine synthetase adenylyltransferase (ATase, EC 2.7.7.49) of Escherichia coli. *Biochemistry* **46**, 4117-4132 (2007).
4. E. R. Stadtman, U. Mura, P. B. Chock, S. G. Rhee, in *Glutamine: Metabolism, Enzymology, and Regulation*, J. Mora, R. Palacios, Eds. (Academic Press, 1980), pp. 41-59.
5. Y. Wang, F. Liu, W. Wang, Kinetics of transcription initiation directed by multiple cis-regulatory elements on the glnAp2 promoter. *Nucleic Acids Research* **44**, 10530-10538 (2016).
6. L. F. Huergo *et al.*, Regulation of glnB gene promoter expression in Azospirillum brasilense by the NtrC protein. *FEMS Microbiol Lett* **223**, 33-40 (2003).
7. L. F. Huergo *et al.*, PII signal transduction proteins: pivotal players in post-translational control of nitrogenase activity. *Microbiology* **158**, 176-190 (2012).
8. V. R. Moure *et al.*, The ammonium transporter AmtB and the PII signal transduction protein GlnZ are required to inhibit DraG in Azospirillum brasilense. *The FEBS Journal* **0**, (2019).
9. V. R. Moure *et al.*, The Nitrogenase Regulatory Enzyme Dinitrogenase Reductase ADP-Ribosyltransferase (DraT) Is Activated by Direct Interaction with the Signal Transduction Protein GlnB. *Journal of Bacteriology* **195**, 279-286 (2013).
10. V. R. Moure *et al.*, in *Endogenous ADP-Ribosylation*, F. Koch-Nolte, Ed. (Springer International Publishing, Cham, 2015), pp. 89-106.
11. Y. Zhang, E. L. Pohlmann, G. P. Roberts, GlnD Is Essential for NifA Activation, NtrB/NtrC-Regulated Gene Expression, and Posttranslational Regulation of Nitrogenase Activity in the Photosynthetic, Nitrogen-Fixing Bacterium Rhodospirillum rubrum. *Journal of Bacteriology* **187**, 1254-1265 (2005).
12. R. Little, I. Martinez-Argudo, R. Dixon, Role of the central region of NifL in conformational switches that regulate nitrogen fixation. *Biochem Soc Trans* **34**, 162-164 (2006).
13. M. McMillan, L. Pereg, Evaluation of reference genes for gene expression analysis using quantitative RT-PCR in Azospirillum brasilense. *PLoS One* **9**, e98162 (2014).
14. M. W. Pfaffl, A new mathematical model for relative quantification in real-time RT-PCR. *Nucleic acids research* **29**, e45-e45 (2001).
15. B. Aquino *et al.*, Effect of point mutations on Herbaspirillum seropedicae NifA activity. *Brazilian Journal of Medical and Biological Research* **48**, 683-690 (2015).
16. K. Miyazaki, Molecular engineering of a PheS counterselection marker for improved operating efficiency in Escherichia coli. *Biotechniques* **58**, 86-88 (2015).
17. F. Sainsbury, E. C. Thuenemann, G. P. Lomonossoff, pEAQ: versatile expression vectors for easy and quick transient expression of heterologous proteins in plants. *Plant Biotechnol J* **7**, 682-693 (2009).
18. V. Oke, S. R. Long, Bacterial genes induced within the nodule during the Rhizobium-legume symbiosis. *Molecular Microbiology* **32**, 837-849 (1999).
19. C. Lou, B. Stanton, Y.-J. Chen, B. Munsky, C. A. Voigt, Ribozyme-based insulator parts buffer synthetic circuits from genetic context. *Nature biotechnology* **30**, 1137-1142 (2012).

20. V. K. Mutalik *et al.*, Precise and reliable gene expression via standard transcription and translation initiation elements. *Nature Methods* **10**, 354 (2013).